



## Segregation of functional networks is associated with cognitive resilience in Alzheimer's disease

Michael Ewers,<sup>1,2</sup> Ying Luan,<sup>1</sup> Lukas Frontzkowski,<sup>1</sup> Julia Neitzel,<sup>1</sup> Anna Rubinski,<sup>1</sup> Martin Dichgans,<sup>1,2,3</sup> Jason Hassenstab,<sup>4,5,6</sup> Brian A. Gordon,<sup>4,5,6</sup> Jasmeer P. Chhatwal,<sup>7</sup> Johannes Levin,<sup>2,8</sup> Peter Schofield,<sup>9,10</sup> Tammie L. S. Benzinger,<sup>4,11</sup> John C. Morris,<sup>4,5,12</sup> Alison Goate,<sup>13,14</sup> Celeste M. Karch,<sup>4,12,15</sup> Anne M. Fagan,<sup>4,5,15</sup> Eric McDade,<sup>4,5</sup> Ricardo Allegri,<sup>16</sup> Sarah Berman,<sup>17</sup> Helena Chui,<sup>18,19</sup> Carlos Cruchaga,<sup>5,12,15,20</sup> Marty Farlow,<sup>21</sup> Neill Graff-Radford,<sup>22</sup> Mathias Jucker,<sup>23,24,25</sup> Jae-Hong Lee,<sup>26</sup> Ralph N. Martins,<sup>27,28,29,30</sup> Hiroshi Mori,<sup>31</sup> Richard Perrin,<sup>4,15,32</sup> Chengjie Xiong,<sup>4,33</sup> Martin Rossor,<sup>34</sup> Nick C. Fox,<sup>34</sup> Antoinette O'Connor,<sup>34,35</sup> Stephen Salloway,<sup>36</sup> Adrian Danek,<sup>8</sup> Katharina Buerger,<sup>1,2</sup> Randall J. Bateman,<sup>4,5</sup> Christian Habeck,<sup>37</sup> Yaakov Stern<sup>37</sup> and Nicolai Franzmeier<sup>1</sup> for the Alzheimer's Disease Neuroimaging Initiative and the Dominantly Inherited Alzheimer Network

Cognitive resilience is an important modulating factor of cognitive decline in Alzheimer's disease, but the functional brain mechanisms that support cognitive resilience remain elusive. Given previous findings in normal ageing, we tested the hypothesis that higher segregation of the brain's connectome into distinct functional networks represents a functional mechanism underlying cognitive resilience in Alzheimer's disease.

Using resting-state functional MRI, we assessed both resting-state functional MRI global system segregation, i.e. the balance of between-network to within-network connectivity, and the alternate index of modularity  $Q$  as predictors of cognitive resilience. We performed all analyses in two independent samples for validation: (i) 108 individuals with autosomal dominantly inherited Alzheimer's disease and 71 non-carrier controls; and (ii) 156 amyloid-PET-positive subjects across the spectrum of sporadic Alzheimer's disease and 184 amyloid-negative controls.

In the autosomal dominant Alzheimer's disease sample, disease severity was assessed by estimated years from symptom onset. In the sporadic Alzheimer's sample, disease stage was assessed by temporal lobe tau-PET (i.e. composite across Braak stage I and III regions). In both samples, we tested whether the effect of disease severity on cognition was attenuated at higher levels of functional network segregation. For autosomal dominant Alzheimer's disease, we found higher functional MRI-assessed system segregation to be associated with an attenuated effect of estimated years from symptom onset on global cognition ( $P = 0.007$ ). Similarly, for patients with sporadic Alzheimer's disease, higher functional MRI-assessed system segregation was associated with less decrement in global cognition ( $P = 0.001$ ) and episodic memory ( $P = 0.004$ ) per unit increase of temporal lobe tau-PET. Confirmatory analyses using the alternate index of modularity  $Q$  revealed consistent results.

In conclusion, higher segregation of functional connections into distinct large-scale networks supports cognitive resilience in Alzheimer's disease.

Received September 2, 2020. Revised November 26, 2020. Accepted December 29, 2020. Advance access publication March 16, 2021

© The Author(s) (2021). Published by Oxford University Press on behalf of the Guarantors of Brain. All rights reserved.

For permissions, please email: journals.permissions@oup.com

- 1 Institute for Stroke and Dementia Research, University Hospital, Ludwig-Maximilian-University LMU, Munich, Germany
- 2 German Center for Neurodegenerative Diseases (DZNE), Munich, Germany
- 3 Munich Cluster for Systems Neurology, SyNergy, Ludwig-Maximilian-University LMU, Munich, Germany
- 4 Knight Alzheimer's Disease Research Center, Washington University in St. Louis, St. Louis, MO, USA
- 5 Department of Neurology, Washington University in St. Louis, St. Louis, MO, USA
- 6 Department of Psychological and Brain Sciences, Washington University, St. Louis, MO, USA
- 7 Massachusetts General Hospital, Department of Neurology, Harvard Medical School, MA, USA
- 8 Department of Neurology, Ludwig-Maximilians-Universität München, Munich, Germany
- 9 Neuroscience Research Australia, Sydney, NSW, Australia
- 10 School of Medical Sciences, University of New South Wales, Sydney, NSW, Australia
- 11 Department of Radiology, Washington University in St. Louis, St. Louis, MO, USA
- 12 Department of Psychiatry, Washington University in St. Louis, St. Louis, MO, USA
- 13 Department of Genetics and Genomic Sciences, Icahn School of Medicine at Mount Sinai, New York, NY, USA
- 14 Ronald M. Loeb Center for Alzheimer's Disease, Department of Neuroscience, Icahn School of Medicine at Mount Sinai, New York, NY, USA
- 15 Hope Center for Neurological Disorders, Washington University in St. Louis, St. Louis, MO, USA
- 16 Department of Neurology, FLENI Foundation, Buenos Aires, Argentina
- 17 Department of Neurology, University of Pittsburgh, Pittsburgh, PA, USA
- 18 Alzheimer's Disease Research Center, Keck School of Medicine at the University of Southern California, Los Angeles, CA, USA
- 19 Department of Neurology, Keck School of Medicine, University of Southern California, Los Angeles, CA, USA
- 20 NeuroGenomics and Informatics, Washington University School of Medicine, St. Louis, MO, USA
- 21 Department of Neurology, Indiana University School of Medicine, Indianapolis, IN, USA
- 22 Department of Neurology, Mayo Clinic, Jacksonville, FL, USA
- 23 German Center for Neurodegenerative Diseases (DZNE), Tübingen, Germany
- 24 Department of Cellular Neurology, Hertie Institute for Clinical Brain Research, Tübingen, Germany
- 25 Department of Psychiatry and Psychotherapy, University of Tübingen, Tübingen, Germany
- 26 Department of Neurology, Asan Medical Center, University of Ulsan College of Medicine, Seoul, Korea
- 27 Centre of Excellence for Alzheimer's Disease Research and Care, School of Medical and Health Sciences, Edith Cowan University, Joondalup, WA, Australia
- 28 Australian Alzheimer's Research Foundation, Ralph and Patricia Sarich Neuroscience Research Institute, Nedlands, WA, Australia
- 29 Department of Biomedical Sciences, Macquarie University, Sydney, NSW, Australia
- 30 KaRa Institute of Neurological Diseases, Sydney, NSW, Australia
- 31 Department of Clinical Neuroscience, Osaka City University Medical School, Osaka, Japan
- 32 Department of Pathology and Immunology, Washington University School of Medicine, St. Louis, MO, USA
- 33 Department of Biostatistics, Washington University, St. Louis, MO, USA
- 34 Dementia Research Centre, University College London, Queen Square, London, UK
- 35 UK Dementia Research Institute at UCL, UCL, London, UK
- 36 Department of Neurology, Warren Alpert Medical School of Brown University, Providence, RI, USA
- 37 Cognitive Neuroscience Division, Department of Neurology, Columbia University, New York, NY, USA

Correspondence to: Michael Ewers  
 Institute for Stroke and Dementia Research  
 Klinikum der Universität München  
 Feodor-Lynenstr. 17, 81377 München, Germany  
 E-mail: michael.ewers@med.uni-muenchen.de

**Keywords:** modularity; resilience; reserve; system segregation; tau-PET

**Abbreviations:** ADAD = autosomal dominant Alzheimer's disease; ADNI = Alzheimer's Disease Neuroimaging Initiative; DIAN = Dominantly Inherited Alzheimer Network; EYO = estimated years from symptom onset; rs-fMRI = resting state functional MRI; SyS = system segregation

## Introduction

Cognitive resilience is defined as the ability to maintain cognitive abilities relatively well in the presence of age-related brain decline or brain pathologies.<sup>1,2</sup> In Alzheimer's disease, the level of cognitive impairment shows substantial variability even when accounting

for key pathologies including amyloid- $\beta$  and pathological tau.<sup>3,4</sup> Protective environmental factors such as education, midlife activities and physical activity have been found to be associated with lower cognitive impairment and dementia risk in Alzheimer's disease,<sup>5-7</sup> suggesting that cognitive resilience may modulate the impact of

pathology on cognition. However, the functional brain properties underlying cognitive resilience remain elusive. Answering that question may help identify and target brain mechanisms that slow down cognitive decline in the presence of Alzheimer's disease pathology. Enhancing cognitive resilience to delay the onset of dementia as much as by 1 year would translate into an age-dependent decrease in dementia prevalence of over 10%.<sup>8</sup>

Previous neuroimaging studies have reported several brain features associated with cognitive resilience in Alzheimer's disease,<sup>9</sup> including higher functional connectivity of hubs in the cognitive control and salience network<sup>10–14</sup> or higher glucose metabolism and brain activation of the anterior cingulate and temporal cortex.<sup>15–17</sup> These findings provide valuable insight into particular brain regions contributing to cognitive resilience in Alzheimer's disease, but overall those regional findings are diverse and variable across studies.<sup>9</sup> There is currently a lack of understanding of which differences in the global functional brain topology support cognitive resilience. From a clinical point of view, a single easily accessible measure of global brain function linked to cognitive resilience would be attractive as a mechanistic functional marker of cognitive resilience.<sup>18</sup> Here we propose resting-state functional MRI (rs-fMRI) assessed segregation between functional networks (called systems) as a putative neural substrate of cognitive resilience. The brain is composed of intrinsically wired functional networks,<sup>19,20</sup> where each network corresponds to a set of tightly connected regions.<sup>20,21</sup> Such a modular functional organization of the brain in the form of clearly segregated functional networks is a critical feature of the functional connectome underlying cognitive performance.<sup>22–24</sup> Multiple graph theoretical indices have been proposed to quantify the segregation of networks.<sup>25</sup> Here, we focus on the statistic called system segregation (SyS), which quantifies the extent to which major functional networks are segregated from each other (i.e. high within-network but low between-network connectivity).<sup>26</sup> An alternative index is the modularity statistic  $Q$ , which quantifies extent to which the clustering of connections into networks deviates from that expected in a randomly connected brain.<sup>22</sup> We chose SyS as our primary predictor because this metric is best suited to quantify the segregation between predefined major resting state networks and thus allows for a clear reference to previously well-characterized functional networks.<sup>27</sup> Results from rs-fMRI studies show higher SyS to be associated with higher global cognitive performance across the adult life span.<sup>26,28</sup> However, few studies have assessed SyS in relation to cognitive resilience. The proxy measure of cognitive resilience including higher socioeconomic status<sup>29,30</sup> was previously found to be associated with higher SyS in normal ageing.<sup>31</sup> In patients with brain injury, higher SyS was associated with better post-recovery cognitive performance,<sup>32</sup> suggesting that SyS confers higher resilience against the impact of brain pathology on cognitive function. Despite these previous findings, to our knowledge no study has yet assessed SyS as a substrate of cognitive resilience in Alzheimer's disease. Here we tested whether higher rs-fMRI-assessed SyS attenuates the association between markers of Alzheimer's disease severity and cognitive decline in two different samples of individuals with genetic or biomarker evidence of Alzheimer's disease. To enhance criterion validity of our analyses, we also tested the alternate modularity index  $Q$  as a predictor of cognitive resilience.

## Materials and methods

### Participants

#### Dominantly Inherited Alzheimer Network

We included 108 carriers of autosomal dominant Alzheimer's disease (ADAD) disease-causing mutations in genes *PSEN1*, and *PSEN2* or *APP*, and 71 non-carrier siblings from Dominantly

Inherited Alzheimer Network (DIAN) data freeze 10.<sup>33</sup> Beyond DIAN inclusion criteria, the current study required availability of 3 T rs-fMRI, T<sub>1</sub> structural MRI and cognitive assessments. No selection bias (i.e. demographic differences between the included participants and excluded participants) was found ( $P > 0.05$ ) for age, gender or education. As a proxy of Alzheimer's disease severity, we applied the estimated years from symptom onset (EYO), defined as the difference between a participants age at examination and the parental age of symptom onset for ADAD mutation carriers, as described previously.<sup>10,34,35</sup> We did not use biomarker levels of pathological tau (as we did in ADNI, see below), since neither CSF biomarkers of tau nor tau PET were available in all subjects in DIAN. Each participant provided written informed consent. Local ethical approval was obtained at each DIAN site.

#### Alzheimer's Disease Neuroimaging Initiative

For the evaluation of late-onset Alzheimer's disease, we included data from the 340 participants included in Alzheimer's Disease Neuroimaging Initiative (ADNI) phase 3, which were selected based on availability of T<sub>1</sub>-weighted and rs-fMRI, <sup>18</sup>F-AV1451 tau-PET for the assessment of tau and <sup>18</sup>F-AV45 amyloid-PET for the assessment of amyloid deposition. All measures had to be obtained at the same study visit. Using Freesurfer-derived global amyloid-PET standardized uptake value ratio (SUVR) scores normalized to the whole cerebellum (provided by the ADNI-PET Core), all participants were characterized as amyloid- $\beta$ -positive or -negative based on an established cut-off point (global AV45 SUVR > 1.11).<sup>36</sup> As a control group, we included 184 cognitively normal [Mini-Mental State Examination (MMSE) > 24, clinical dementia rating (CDR) = 0, non-depressed] amyloid- $\beta$ -negative participants. To cover the Alzheimer's continuum, we included 89 cognitively normal amyloid- $\beta$ -positive participants, 59 mild cognitively impaired amyloid- $\beta$ -positive participants (MMSE > 24, CDR = 0.5, objective memory-loss on the education adjusted Wechsler Memory Scale II, preserved activities of daily living) and eight amyloid- $\beta$ -positive patients with dementia (MMSE < 26, CDR > 0.5, fulfilment of NINCDS/ADRDA criteria for probable Alzheimer's disease).<sup>37</sup> Region of interest-specific AV1451 tau-PET data for Freesurfer-based Desikan-Killiany regions of interest provided by the ADNI PET-Core were downloaded from the online ADNI image archive (<https://ida.loni.usc.edu>). As a proxy of disease severity in sporadic Alzheimer's disease, tau-PET uptake averaged across Braak-stage regions of interest I and III was assessed according to a previously described protocol.<sup>38</sup> We specifically focused on these early Braak-stage regions of interest to enhance sensitivity to tau accumulation during the early stages of Alzheimer's disease. We excluded the hippocampus (i.e. Braak-stage-II region of interest) because of known susceptibility of AV1451 PET measures in the hippocampal region to spill-over effects of off-target AV1451 binding in the neighbouring choroid plexus.<sup>39</sup> Ethical approval was obtained by the ADNI investigators, all participants provided written informed consent.

#### Neuropsychology

In DIAN, we used a pre-established z-score composite score of global cognition, which was designed by the DIAN cognitive core based on the tests' low ceiling/floor effects, high face validity and sensitivity to early Alzheimer's disease, and is included as the primary end point in the DIAN clinical trial.<sup>40</sup> For the assessment of episodic memory, a memory composite was generated, which was defined as the average z-score (i.e. normalized to the full DIAN baseline sample of cognitively normal non-mutation carriers) across all memory scores available in DIAN (i.e. Wechsler Memory Scale-Revised, Story A logical memory immediate and delayed

recall, immediate and delayed recall of a 16-item word list, and an associative memory test). These tests were chosen due to their sensitivity to cognitive changes in early stage ADAD subjects (at CDR score = 0.05) as previously described.<sup>41</sup> For ADNI participants, we used the total score of the ADAS13 for global cognition and the pre-established composite memory score ADNI-MEM,<sup>42</sup> which is a widely used composite scores of cognition in ADNI,<sup>43</sup> and thus offers high comparability between studies. As expected, measures of global cognition and memory were correlated within each cohort (DIAN:  $r = 0.81$ ,  $P < 0.001$ ; ADNI:  $r = -0.85$ ,  $P < 0.001$ ).

### MRI acquisition and preprocessing

In all samples, MRI data were obtained on 3 T scanner systems. Structural MRI was obtained in both samples using a 3D  $T_1$ -weighted magnetization prepared rapid acquisition gradient echo (MPRAGE) sequence (ADNI: 1 mm isotropic voxel-size, repetition time = 2300 ms; DIAN  $1.1 \times 1.1 \times 1.2$  mm voxel-size, repetition time = 2300 ms). In ADNI, 200 rs-fMRI volumes were obtained using a  $T_2^*$ -weighted EPI sequence with 3.4 mm isotropic voxel resolution with a repetition time/echo time/flip angle = 3000 ms/30 ms/90°. In DIAN, 140 rs-fMRI volumes were collected also using a  $T_2^*$ -weighted echo planar imaging (EPI) sequence with a TR/TE/flip angle = 2230ms/30 ms/80°. All rs-fMRI images were preprocessed and spatially normalized using the same SPM12-based (Wellcome Trust Centre for Neuroimaging, University College London) pipeline using DARTEL as described previously.<sup>10,13,14</sup> Rs-fMRI preprocessing further included motion correction, detrending, band-pass filtering (0.01–0.08 Hz), nuisance regression (i.e. six motion parameters, mean signal extracted from CSF and white matter masks), motion scrubbing and spatial smoothing using an 8 mm full-width at half-maximum Gaussian kernel. Motion scrubbing followed a pre-established approach, where we computed frame-wise displacement between adjacent fMRI volumes. Volumes that exceeded a frame-wise displacement threshold  $>0.5$  mm were censored (i.e. replaced with zero-padded volumes) together with one preceding and two subsequent volumes. No subjects were included for which  $>30\%$  of the resting-state scan had to be removed during motion scrubbing. There were no differences in the average percentage of censored volumes (ADNI:  $6 \pm 11\%$ ; DIAN  $7 \pm 10\%$ ) between amyloid- $\beta$ -positive versus amyloid- $\beta$ -negative in ADNI or between mutation carriers versus non-carriers in DIAN (all  $P > 0.05$ ). Note that all the above described image processing steps were conducted independently in DIAN and ADNI, hence no data were merged between the two cohorts during any stage of data processing or analysis.

### Assessment of functional connectivity and system segregation

Functional connectivity was estimated in a region of interest-based manner, using 400 regions of interest from the Schaefer fMRI atlas (Fig. 1) which covers the neocortex.<sup>44</sup> The 400 regions are grouped within seven large-scale functional networks (Fig. 1A) in line with previous parcellations.<sup>45</sup> Prior to all analyses, the Schaefer fMRI atlas was masked with sample-specific grey matter masks (i.e. voxels with at least 30% probability of belonging to grey matter within the ADNI or BioFINDER sample). Interregional functional connectivity was estimated for each subject based on the fully preprocessed fMRI data. Specifically, we extracted the mean fMRI time series for each of the 400 regions of interest by averaging the signal across voxels falling within a given region. Mean region of interest time series were then cross-correlated using Pearson-Moment correlation, yielding a  $400 \times 400$  functional connectivity matrix that was subsequently Fisher z-transformed.

Autocorrelations were set to zero and only positive connections were retained. System segregation was computed for each of the seven networks from a previously established network parcellation<sup>44</sup> as the difference between mean within network functional connectivity and mean functional connectivity of the network nodes to the remaining six networks (i.e. between-network functional connectivity), as:

$$SyS = \frac{\bar{z}_w - \bar{z}_b}{\bar{z}_w} \quad (1)$$

where  $\bar{z}_w$  is the mean connectivity of all nodes within a given network and  $\bar{z}_b$  is the mean connectivity of all nodes of a given network to nodes outside of that network.<sup>26</sup> Global SyS was computed as the mean segregation across all seven networks and used for subsequent analyses.

To ensure that our analyses were not driven by the selection of a particular graph-metric, we additionally computed the modularity coefficient  $Q$ ,<sup>46</sup> which is an alternative measure to quantify the segregation of brain networks, using the following equation:

$$Q = \frac{1}{2m} \sum_{ij} \left[ A_{ij} - \frac{k_i k_j}{2m} \right] \delta(c_i, c_j) \quad (2)$$

where  $A_{ij}$  represents the connectivity between nodes  $i$  and  $j$ ,  $k_i$  and  $k_j$  are the sum of the connectivity weights attached to nodes  $i$  and  $j$ ,  $m$  is the sum of all connectivity weights in the graph,  $c_i$  and  $c_j$  are the communities of the nodes and  $\delta$  is the Kronecker delta function. SyS and  $Q$  were highly correlated in both cohorts (DIAN:  $r = 0.9$ ,  $R^2 = 0.81$ ,  $P < 0.001$ ; ADNI:  $r = 0.86$ ,  $R^2 = 0.74$ ,  $P < 0.001$ ), supporting the notion that both metrics assess the same underlying construct of brain network segregation.

### Statistics

For DIAN, baseline demographic scores were compared between mutation-carriers and non-carriers using t-tests for continuous and  $\chi^2$  tests for nominal variables. For the ADNI sample, demographics were compared between diagnostic groups using ANOVAs for continuous variables and  $\chi^2$  for nominal variables.

In DIAN, we first tested whether higher EYO was associated with worse cognitive performance (i.e. global cognitive and memory composite), using linear mixed models, controlling for age, gender, education (fixed effects), family affiliation and random intercept

### 400 ROI Brain parcellation

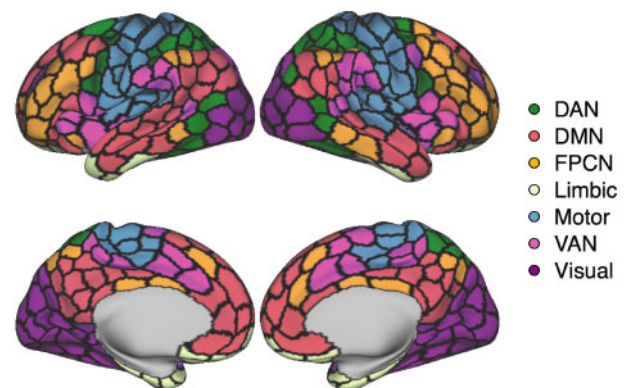


Figure 1 Functional brain parcellation. 400-ROI Brain parcellation that was used to determine functional connectivity and system segregation between brain networks.<sup>44</sup>

(random effects). For our major hypothesis, we assessed next whether higher SyS attenuated the association between advanced EYO and cognitive performance in the ADAD mutation carriers. To this end, we used linear mixed models to test the interaction between SyS and EYO on cognition (i.e. global cognitive and memory composite), again controlling for age, gender, education, mean motion (i.e. framewise displacement) during the rs-fMRI scan (fixed effects), family affiliation and random intercept (random effects). For analyses in DIAN, we used a Bonferroni-corrected alpha threshold of 0.025 (i.e.  $\alpha = 0.05$  adjusted for two tests, that is one test on global cognition, the other on memory performance).

In the ADNI tau-PET sample, we used tau-PET in Braak-stage I and III regions as markers of early core Alzheimer's disease pathology. We preferred tau-PET over amyloid PET as a marker of disease progression, given tau-PET's superior correlation with neurodegeneration and cognitive decline in Alzheimer's disease.<sup>47,48</sup> We first tested whether a higher tau-PET SUVR (i.e. Braak I+III composite) was associated with worse cognition (i.e. ADAS13 for global cognition and ADNI-MEM for memory performance), using linear mixed models controlling for age, gender, education, mean motion (i.e. framewise displacement) during the rs-fMRI scan (fixed effects), study centre and random intercept (random effects). Next, we again tested our major hypothesis whether higher SyS attenuated the effect of Braak I+III tau-PET SUVR on ADAS13/ADNI-MEM (i.e. SyS  $\times$  Braak I+III tau-PET interaction) using linear mixed models, and controlling for age, gender, education, mean motion (i.e. framewise displacement) during the rs-fMRI scan (fixed effects), study centre and random intercept (random effects). As in DIAN, we used a Bonferroni-corrected alpha threshold of 0.025, adjusting for two tests. To ensure that the above described analyses were not driven by the selection of SyS as a graph metric, we repeated the analyses using the modularity coefficient Q (as implemented in the R toolbox phenoClust) as an alternative measure of network segregation. All statistical analyses were performed in R statistical software (version 3.6.1).

## Data availability

The data that support the findings of this study are available from the corresponding author for the purpose of replication upon request.

## Results

Baseline subject characteristics are displayed in Table 1. When comparing SyS scores between Alzheimer's disease groups and controls, there was no difference in SyS between mutation-carriers and the non-carrier group ( $F = 2.388$ ,  $P = 0.124$ ; Fig. 2A) of the DIAN sample. In ADNI, however, we found decreased SyS in amyloid- $\beta$ -positive as compared to amyloid- $\beta$ -negative participants ( $F = 8.904$ ,  $P = 0.003$ ; Cohen's  $d = -0.478$ ; Fig. 2B).

### System segregation attenuates cognitive deficits in familial Alzheimer's disease

As a proxy of ADAD disease severity, we used EYO, which is associated with performance on measures of both global cognition ( $\beta = -0.657$ , Cohen's  $d = -1.834$ ,  $P < 0.001$ ) and memory ( $\beta = -0.590$ , Cohen's  $d = -1.376$ ,  $P < 0.001$ ) as shown by linear mixed effects models controlling for age, gender, education (fixed effects) and family affiliation and random intercept (random effects). To test our major hypothesis, we determined the interaction effect between system segregation and EYO on either global cognition or memory, controlling for gender, education, mean motion during the rs-fMRI scan (i.e. framewise displacement; fixed effects), family affiliation and random intercept (random effects). As hypothesized, we found a SyS segregation by EYO interaction on global cognition ( $\beta = 0.209$ ,  $P = 0.007$ , Cohen's  $d = 0.57$ ; Fig. 3A), such that ADAD mutation-carriers with higher SyS had better global cognitive performance at a given level of EYO compared to ADAD mutation-carriers with lower SyS. The interaction effect remained significant after accounting for multiple testing. Testing the same interaction effect for memory performance, however, yielded non-significant results ( $\beta = 0.026$ ,  $P = 0.799$ , Cohen's  $d = -0.055$ ; Fig. 3B). Using the modularity coefficient Q instead of SyS yielded consistent interaction effects with EYO on global cognition ( $\beta = 0.209$ ,  $P = 0.004$ , Cohen's  $d = 0.650$ ; Supplementary Fig. 1A) but not memory performance ( $\beta = 0.033$ ,  $P = 0.727$ ; Supplementary Fig. 1B). Together, the analyses in the DIAN cohort suggest that higher segregation of brain networks is associated with attenuated global cognitive decreases in ADAD.

Table 1 Sample characteristics in each group

ADNI	CN A $\beta$ - (n = 184)	CN A $\beta$ + (n = 89)	MCI A $\beta$ + (n = 59)	Alzheimer's disease dementia (n = 8)	P-value
Age	72.3 (6.8)	75.8 (6.6)	76.3 (7.5)	73.5 (11.5)	<0.001
Gender, female/male	112/72	56/33	25/34	3/5	0.033
Education	16.9 (2.3)	16.4 (2.5)	15.8 (2.7)	16.3 (2.3)	0.010
ADAS13	12.2 (4.6)	13.6 (5.6)	22.8 (10.5)	31.7 (8.6)	<0.001
DIAN	Non-carrier (n = 71)	Mutation-carrier (n = 108)			
Age	38.1 (10.3)	38.0 (10.5)			0.953
EYO	-9.8 (11.0)	-8.6 (11.2)			0.470
Gender, female/male	44/27	68/40			0.990
Education	15.2 (3.1)	14.2 (3.3)			0.033
Global cognitive composite	0.19 (0.2)	-0.15 (0.5)			<0.001

The classification of amyloid- $\beta$ -positive (A $\beta$ +) or amyloid- $\beta$ -negative (A $\beta$ -) status was based on a previously established cut-off point (global AV45 SUVR > 1.11).<sup>36</sup> For continuous measures, the mean (SD) are displayed. CN = cognitively normal; MCI = mild cognitive impairment.

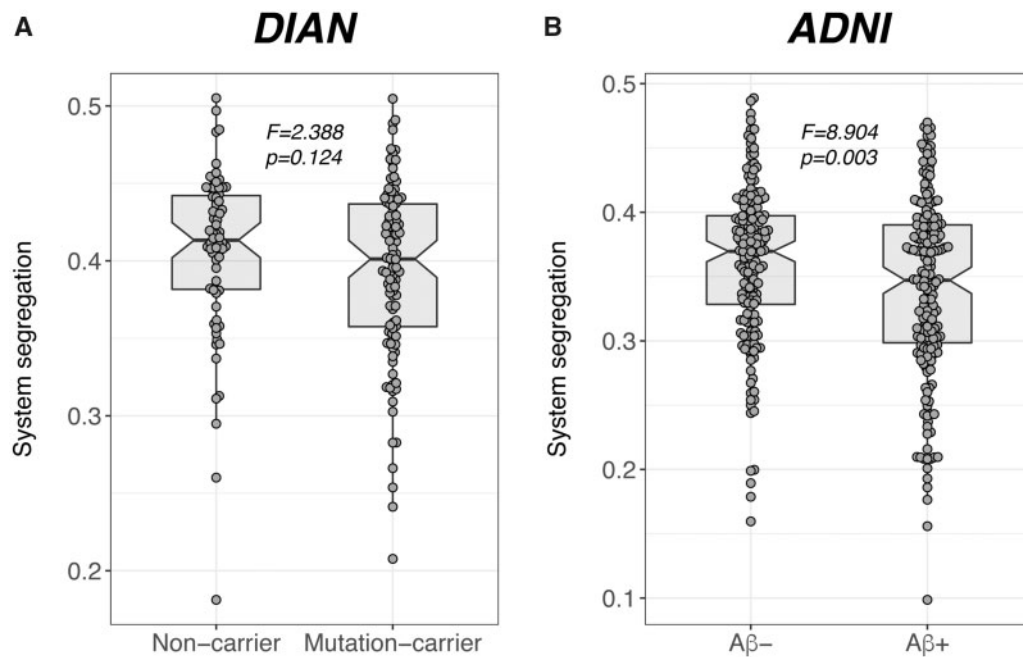


**Figure 2** Group differences in SyS. Group differences in system segregation between controls and patients with autosomal dominant (DIAN) and sporadic (ADNI) Alzheimer's disease.

### System segregation is associated with cognitive resilience in sporadic Alzheimer's disease

We aimed to assess whether beneficial effects of SyS on cognition are also evident in the more common sporadic form of Alzheimer's disease. To this end, we tested in 156 amyloid- $\beta$ -positive ADNI participants whether higher SyS was associated with attenuated effects of primary Alzheimer's disease pathology on cognition. As a measure of primary Alzheimer's disease pathology that is strongly linked to cognition, we used a composite tau-PET SUVR score, summarizing tau-PET levels within Braak stage-specific regions of interest I and III. The tau-PET composite of Braak-stage regions of interest I and III was significantly higher in the amyloid- $\beta$ -positive group than in the amyloid- $\beta$ -negative group ( $F = 51.69$ ,  $P < 0.001$ , Cohen's  $d = 0.809$ , ANCOVA controlled for age, gender and education), and higher tau-PET composite scores were strongly associated with worse global cognition (i.e. ADAS13 total score,  $\beta = 0.26$ , Cohen's  $d = 0.613$ ,  $P < 0.001$ ) and memory (i.e. ADNI-MEM,  $\beta = -0.372$ , Cohen's  $d = -0.622$ ,  $P < 0.001$ ) in the amyloid- $\beta$ -positive group [linear mixed models controlling for age, gender, education (fixed effects), study centre and random intercept (random effects)]. Analogous to our analyses in DIAN, we then tested the interaction between SyS and the tau-PET composite on global cognition (i.e. ADAS13 total score) memory (i.e. ADNI-MEM), controlling for age, gender, education, diagnosis and mean framewise displacement (fixed effects) as well as study centre and random intercept (random effects). We found significant SyS by tau-PET composite interactions on both global cognition ( $\beta = -0.268$ ,  $P < 0.001$ , Cohen's  $d = -0.569$ ; Fig. 3C) and memory performance ( $\beta = 0.220$ ,  $P = 0.004$ , Cohen's  $d = 0.488$ ; Fig. 3D). Both interaction effects remained significant after accounting for multiple testing. As shown in Fig 3C and D, higher SyS was associated with less severe global cognitive and memory impairment as a function of tau-PET. Tau-PET was not associated with lower SyS in ADNI amyloid- $\beta$ -positive subjects. Repeating the above described analyses with the modularity coefficient  $Q$  (i.e. tau-PET by modularity interaction), yielded consistent results for global cognition ( $\beta = -0.175$ ,  $P = 0.021$ , Cohen's  $d = -0.393$ ; Supplementary Fig. 1C) and memory

( $\beta = 0.180$ ,  $P = 0.015$ , Cohen's  $d = 0.413$ ; Supplementary Fig. 1D). The modularity index  $Q$  was not associated with tau PET ( $P > 0.05$ ). When exploratorily repeating the analyses in the amyloid- $\beta$ -negative group, no significant tau-PET composite by SyS or tau-PET composite by modularity interaction effects were found (all  $P > 0.05$ ; Supplementary Fig. 2), suggesting that effects were restricted to the amyloid- $\beta$ -positive group. We caution, however, that the current study was not intended to test associations between tau and cognition in normal ageing, thus the analyses in the amyloid- $\beta$ -negative group are exploratory and should not be regarded as evidence that SyS does not attenuate age-related cognitive changes. Together, our findings support the hypothesis that higher segregation of brain networks supports higher cognitive performance in the face of Alzheimer's disease pathology.

### Discussion

We found that higher rs-fMRI-assessed SyS was associated with attenuated cognitive deficits in ADAD and sporadic Alzheimer's disease, such that higher SyS predicted a lower impact of disease progression markers (including EYO and tau PET) on cognitive performance. All findings were replicated with the modularity coefficient  $Q$ , i.e. an alternative graph metric for segregation between brain networks. Although our findings do not imply that the segregation of brain networks has a causative effect, these results strongly support a protective role of SyS on cognitive changes during the course of Alzheimer's disease.

SyS was associated with an altered effect of core Alzheimer's disease progression markers on cognition, providing the first evidence that higher SyS is not only associated with higher cognition in normal ageing as shown previously,<sup>26,28</sup> but also with higher cognitive resilience in Alzheimer's disease. We found the same pattern of results when using the alternate index of modularity  $Q$ . Although computationally different, both indices are conceptually closely related by quantifying the extent to which functional connections segregate into densely connected networks.<sup>27</sup> Thus, across different graph theoretical indices, we found that higher

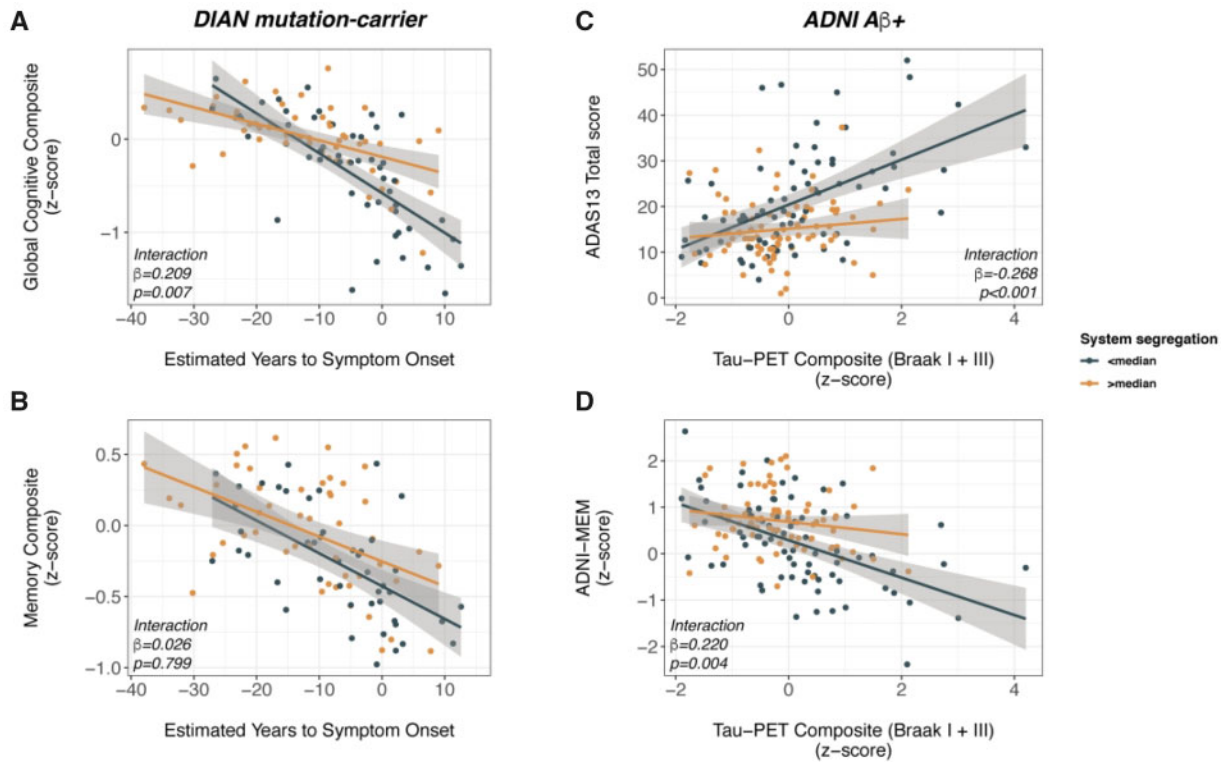


**Figure 3** System segregation moderates the association between Alzheimer's disease severity and cognition. Interaction effect of system segregation by disease progression markers on cognitive performance in autosomal dominant (A and B) and sporadic Alzheimer's disease (C and D). Note that interaction effects were determined using continuous values of system segregation, while median splits are for illustrational purposes only. Note that higher scores on the ADAS13 (C) indicates worse cognition, whereas higher scores on the composite measures (A, B and D) indicate better cognition.

segregation of networks is associated with enhanced cognitive resilience. We validated our findings across different cohorts including ADAD and sporadic Alzheimer's disease. ADAD provides a unique opportunity to study cognitive resilience-related mechanisms in Alzheimer's disease, where the confounding influence of age-related pathologies such as hypertensive cerebrovascular disease are unlikely due to early disease onset.<sup>49</sup> However, although pathological brain alterations in ADAD are largely comparable to those in sporadic late-onset Alzheimer's disease,<sup>34,49,50</sup> there are important differences. Compared to sporadic Alzheimer's disease, ADAD is associated with greater subcortical deposition of amyloid- $\beta$  and higher occurrence of atypical 'cotton wool' amyloid plaques.<sup>51</sup> Therefore, the validation of our findings on the protective effects of SyS in sporadic Alzheimer's disease is important. Together, these results provide evidence for a protective role of SyS in Alzheimer's disease regardless of disease aetiology.

In the current study, SyS was slightly reduced in participants with biomarker evidence of sporadic Alzheimer's disease but not ADAD, however the overlap in SyS was large in ADNI between the Alzheimer's disease and non-Alzheimer's disease groups. One possible explanation for the inconsistency between ADNI and DIAN is that not all ADAD individuals yet showed elevated levels of Alzheimer's disease pathology, which may have reduced our power to detect the small Alzheimer's disease-related reduction in SyS. Our results of SyS decreases in sporadic, amyloid- $\beta$ -positive participants are consistent with previous reports of reduced segregation of functional networks in elderly participants with elevated biomarker levels of amyloid- $\beta$ .<sup>52</sup> The reduction of SyS in participants with elevated levels of amyloid- $\beta$  raises the possibility that individuals with higher SyS had simply less severe Alzheimer's disease pathology and thus lower cognitive impairment. However,

we consider this explanation unlikely. Note that we tested the interaction effect of SyS by tau-PET on cognition, where in individuals with higher SyS, the decrease in cognition per unit increase in tau pathology was attenuated. Therefore, the critical test for cognitive resilience was whether SyS was associated with an attenuated effect of tau PET on cognitive impairment rather than the level of tau pathology per se. Moreover, within the group of amyloid-PET positive participants, SyS was not related to amyloid PET levels or tau PET, where SyS was still associated with an attenuated effect of tau PET on cognitive decline. Thus, the association between SyS and cognitive resilience cannot be simply attributed to lower levels of core Alzheimer's disease pathology in individuals with higher SyS.

The specific functional mechanisms that link SyS to higher cognitive performance are not fully understood. A recent theoretical framework suggested that SyS could be regulated by multiple control mechanisms such as hub connectivity in cognitive control networks.<sup>18,53</sup> Higher system segregation is under the tight control of hubs, i.e. highly connected regions that are thought to be central to brain function.<sup>54</sup> In cognitively normal individuals, higher connectivity between hubs and major networks in the brain are associated with higher segregation of functional networks, which, in turn, are associated with higher cognitive performance across different cognitive domains.<sup>53</sup> We and others have previously shown that both higher resting-state and task-related functional connectivity of a global hub in the cognitive control network is associated with higher cognitive resilience.<sup>10,11,13,14,55,56</sup> In addition, functional connectivity and activity of the anterior cingulate, another hub in the brain linked with higher modularity and higher general cognitive function,<sup>57,58</sup> has been repeatedly associated with higher cognitive resilience in ageing and Alzheimer's disease.<sup>17,59</sup>

Together, these findings suggest that higher SyS may be a downstream final pathway of functional topology of the brain that supports cognitive resilience in Alzheimer's disease. It is important to consider that our current results are based on rs-fMRI which may act as a baseline reference of functional brain organization from which task-specific network changes occur.<sup>27,60</sup> Interactions and connectivity between brain networks have been shown to dynamically change during task-demands.<sup>61</sup> In fact, it has been shown that brain network segregation decreases when individuals face novel and difficult tasks, but that network segregation restores during learning of the task. This suggests that mastering a task is associated with increasing system segregation.<sup>62</sup> Thus, it will be a critical next step to assess whether higher resting-state SyS is associated with task-specific network reorganization and cognitive performance. A further open question is whether the interindividual differences in SyS are persistent throughout life and which factors may have caused such differences. Note that we used the term cognitive resilience rather than cognitive reserve in the current study to remain agnostic to varies sources of influence that may have determined or shaped SyS. Life span studies are need to address genetic,<sup>63</sup> life style<sup>64</sup> and age-specific factors<sup>7</sup> that influence SyS.

### Limitations

One limitation is that we assessed SyS based on *a priori* defined large-scale resting-state networks rather than networks/modules defined at the individual level. Network boundaries may change during ageing and disease, and thus the measure of SyS and modularity Q based on predefined networks may be altered due to ill-defined networks. However, large-scale resting state networks have been shown to be highly reproducible in ageing and Alzheimer's disease. A major advantage of choosing canonical resting state networks as the basic units is the increased interpretability of the findings, given the extensive cognitive characterization of such networks.<sup>20</sup> An alternate computation of the modularity index Q is based on a data-driven determination of networks,<sup>65</sup> including the search for the optimal clustering of functional connections. However, the modularity optimization search is a non-deterministic polynomial hard problem,<sup>66</sup> where the optimization depends on multiple parameters without any hard criteria of choosing the best model.<sup>67</sup> Therefore, from a clinical point of view, it is more attractive to resort to *a priori* well-established and cognitively characterized functional networks as the basic units of network analysis.

Another caveat is the question of how stable and reproducible SyS is across time. Functional MRI connectivity estimation can be biased by physiological noise (e.g. respiratory and cardiac signals; vascular changes) and motion artefacts that may limit reliable estimation of SyS or Q.<sup>68,69</sup> To correct for motion artefacts we combined motion correction, motion regression and motion scrubbing, referring to the censoring of high-motion volumes from fMRI data, which has been shown to minimize the influence of motion on connectivity estimation.<sup>68</sup> In addition, we included subject-specific average motion estimates as covariates in second level statistical models to additionally correct the assessment of SyS by tau-PET (ADNI) or SyS by EYO (DIAN) interaction models for motion during the fMRI scan. While the currently employed motion correction pipeline has been motivated by previous work,<sup>68</sup> we would like to acknowledge that other motion-correction methods have been also proposed, including data interpolation, principal component-based denoising etc., and there is currently no 'best' motion-correction pipeline.<sup>70</sup> For physiological noise (e.g. respiratory, cardiac signals and vascular confounds), there were no consistent measures available across the cohorts, hence we encourage future

studies to validate our findings using fMRI data with concurrent physiological recordings or vascular health measures. Regarding test-retest reliability of the currently used fMRI measures, there is a dearth of data for SyS. However, previous studies on the modularity index Q show moderate test-retest variability, which was superior to the reliability of first order interregional connectivity measures,<sup>71</sup> e.g. commonly used pair-wise region of interest-to-region of interest correlations. Importantly, the size of inter-individual differences in modularity exceed that of temporal fluctuations of modularity within an individual,<sup>72</sup> supporting the view that fMRI assessed modularity may serve as a fingerprint of cognitive resilience in participants.

### Conclusions

We demonstrated for the first time that individuals with higher SyS exhibited attenuated cognitive impairment at a given level of Alzheimer's disease pathology. Higher modular organization of the brain may thus play an important role in maintaining relatively well cognitive abilities in the face of Alzheimer's disease pathology. The rs-fMRI-based assessment of SyS provides thus both mechanistic insight into functional brain differences that support cognitive resilience as well as a promising approach to develop a marker to predict progression of cognitive decline in Alzheimer's disease.

### Acknowledgements

We would like to thank all the researchers in the DIAN ([www.dian-info.org/personnel.htm](http://www.dian-info.org/personnel.htm)) and ADNI study. We acknowledge the altruism of the DIAN and ADNI participants and their families.

### Funding

The study was funded by LMUexcellent, the Bavaria-Quebec Foundation (to M.E.), Deutsche Forschungsgemeinschaft (DFG, German Research Foundation) grant for major research instrumentation (DFG, INST 409/193-1 FUGG, to M.D.), and the National Institute for Health Research University College London Hospitals Biomedical Research Centre and the MRC Dementias Platform UK (MR/L023784/1 and MR/009076/1 to M.R.). Data collection and sharing for this project was supported by The Dominantly Inherited Alzheimer's Network (DIAN, U19AG032438) funded by the National Institute on Aging (NIA). Data collection and sharing for this project was funded by the Alzheimer's Disease Neuroimaging Initiative (ADNI) (National Institutes of Health Grant U01 AG024904) and DOD ADNI (Department of Defense award number W81XWH-12-2-0012). ADNI is funded by the National Institute on Aging, the National Institute of Biomedical Imaging and Bioengineering, and through generous contributions from the following: AbbVie, Alzheimer's Association; Alzheimer's Drug Discovery Foundation; Araclon Biotech; BioClinica, Inc.; Biogen; Bristol-Myers Squibb Company; CereSpir, Inc.; Cogstate; Eisai Inc.; Elan Pharmaceuticals, Inc.; Eli Lilly and Company; EuroImmun; F. Hoffmann-La Roche Ltd and its affiliated company Genentech, Inc.; Fujirebio; GE Healthcare; IXICO Ltd ; Janssen Alzheimer Immunotherapy Research & Development, LLC.; Johnson & Johnson Pharmaceutical Research & Development LLC.; Lumosity; Lundbeck; Merck & Co., Inc.; Meso Scale Diagnostics, LLC.; NeuroRx Research; Neurotrack Technologies; Novartis Pharmaceuticals Corporation; Pfizer Inc.; Piramal Imaging; Servier; Takeda Pharmaceutical Company; and Transition Therapeutics. The Canadian Institutes of Health Research is providing funds to support ADNI clinical sites in Canada. Private sector contributions are facilitated by the Foundation for the National Institutes of Health



(www.fnih.org). The grantee organization is the Northern California Institute for Research and Education, and the study is coordinated by the Alzheimer's Therapeutic Research Institute at the University of Southern California. ADNI data are disseminated by the Laboratory for Neuro Imaging at the University of Southern California.

## Competing interests

The authors report no competing interests.

## Supplementary material

Supplementary material is available at *Brain* online.

## References

1. Stern Y, Arenaza-Urquijo EM, Bartres-Faz D, et al. Whitepaper: Defining and investigating cognitive reserve, brain reserve, and brain maintenance. *Alzheimers Dement*. 2020;16(9):1305–1311.
2. Cabeza R, Albert M, Belleville S, et al. Maintenance, reserve and compensation: The cognitive neuroscience of healthy ageing. *Nat Rev Neurosci*. 2018;19(11):701–710.
3. Franzmeier N, Koutsouleris N, Benzinger T, et al.; Dominantly Inherited Alzheimer Network (DIAN). Predicting sporadic Alzheimer's disease progression via inherited Alzheimer's disease-informed machine-learning. *Alzheimers Dement*. 2020;16(3):501–511.
4. Jack CR, Knopman DS, Jagust WJ, et al. Tracking pathophysiological processes in Alzheimer's disease: An updated hypothetical model of dynamic biomarkers. *Lancet Neurol*. 2013;12(2):207–216.
5. Wang HX, MacDonald SW, Dekhtyar S, Fratiglioni L. Association of lifelong exposure to cognitive reserve-enhancing factors with dementia risk: A community-based cohort study. *PLoS Med*. 2017;14(3):e1002251.
6. Dekhtyar S, Marseglia A, Xu W, Darin-Mattsson A, Wang HX, Fratiglioni L. Genetic risk of dementia mitigated by cognitive reserve: A cohort study. *Ann Neurol*. 2019;86(1):68–78.
7. Chan D, Shafto M, Kievit R, et al.; Cam-CAN. Lifestyle activities in mid-life contribute to cognitive reserve in late-life, independent of education, occupation, and late-life activities. *Neurobiol Aging*. 2018;70:180–183.
8. Zissimopoulos J, Crimmins E, St Clair P. The value of delaying Alzheimer's disease onset. *Forum Health Econ Policy*. 2014;18(1):25–39.
9. Ewers M. Reserve in Alzheimer's disease: Update on the concept, functional mechanisms and sex differences. *Curr Opin Psychiatry*. 2020;33(2):178–184.
10. Franzmeier N, Duzel E, Jessen F, et al. Left frontal hub connectivity delays cognitive impairment in autosomal-dominant and sporadic Alzheimer's disease. *Brain*. 2018;141(4):1186–1200.
11. Neitzel J, Franzmeier N, Rubinski A, Ewers M; for the Alzheimer's Disease Neuroimaging Initiative (ADNI). Left frontal connectivity attenuates the adverse effect of entorhinal tau pathology on memory. *Neurology*. 2019;93(4):e347–e357.
12. Benson G, Hildebrandt A, Lange C, et al. Functional connectivity in cognitive control networks mitigates the impact of white matter lesions in the elderly. *Alzheimers Res Ther*. 2018;10(1):109.
13. Franzmeier N, Duering M, Weiner M, Dichgans M, Ewers M; Alzheimer's Disease Neuroimaging Initiative (ADNI). Left frontal cortex connectivity underlies cognitive reserve in prodromal Alzheimer disease. *Neurology*. 2017;88(11):1054–1061.
14. Franzmeier N, Gottler J, Grimmer T, et al. Resting-state connectivity of the left frontal cortex to the default mode and dorsal attention network supports reserve in mild cognitive impairment. *Front Aging Neurosci*. 2017;9:264.
15. Stern Y, Gazes Y, Razlighi Q, Steffener J, Habeck C. A task-invariant cognitive reserve network. *Neuroimage*. 2018;178:36–45.
16. van Loenhoud AC, Habeck C, van der Flier WM, Ossenkoppele R, Stern Y. Identifying a task-invariant cognitive reserve network using task potency. *Neuroimage*. 2020;210:116593.
17. Arenaza-Urquijo EM, Przybelski SA, Lesnick TL, et al. The metabolic brain signature of cognitive resilience in the 80+: beyond Alzheimer pathologies. *Brain*. 2019;142(4):1134–1147.
18. Medaglia JD, Pasqualetti F, Hamilton RH, Thompson-Schill SL, Bassett DS. Brain and cognitive reserve: Translation via network control theory. *Neurosci Biobehav Rev*. 2017;75:53–64.
19. Crossley NA, Mechelli A, Vertes PE, et al. Cognitive relevance of the community structure of the human brain functional coactivation network. *Proc Natl Acad Sci U S A*. 2013;110(28):11583–11588.
20. Smith SM, Fox PT, Miller KL, et al. Correspondence of the brain's functional architecture during activation and rest. *Proc Natl Acad Sci U S A*. 2009;106(31):13040–13045.
21. Cole MW, Bassett DS, Power JD, Braver TS, Petersen SE. Intrinsic and task-evoked network architectures of the human brain. *Neuron*. 2014;83(1):238–251.
22. Sporns O, Betzel RF. Modular brain networks. *Annu Rev Psychol*. 2016;67:613–640.
23. Achard S, Salvador R, Whitcher B, Suckling J, Bullmore E. A resilient, low-frequency, small-world human brain functional network with highly connected association cortical hubs. *J Neurosci*. 2006;26(1):63–72.
24. Bullmore E, Sporns O. The economy of brain network organization. *Nat Rev Neurosci*. 2012;13(5):336–349.
25. Sporns O. Graph theory methods: Applications in brain networks. *Dialogues Clin Neurosci*. 2018;20(2):111–121.
26. Chan MY, Park DC, Savalia NK, Petersen SE, Wig GS. Decreased segregation of brain systems across the healthy adult lifespan. *Proc Natl Acad Sci U S A*. 2014;111(46):E4997–E5006.
27. Wig GS. Segregated systems of human brain networks. *Trends Cogn Sci*. 2017;21(12):981–996.
28. Varangis E, Habeck CG, Razlighi QR, Stern Y. The effect of aging on resting state connectivity of predefined networks in the brain. *Front Aging Neurosci*. 2019;11:234.
29. Chapko D, McCormack R, Black C, Staff R, Murray A. Life-course determinants of cognitive reserve (CR) in cognitive aging and dementia - a systematic literature review. *Aging Ment Health*. 2018;22(8):915–926.
30. Marden JR, Tchetgen Tchetgen EJ, Kawachi I, Glymour MM. Contribution of socioeconomic status at 3 life-course periods to late-life memory function and decline: Early and late predictors of dementia risk. *Am J Epidemiol*. 2017;186(7):805–814.
31. Chan MY, Na J, Agres PF, Savalia NK, Park DC, Wig GS. Socioeconomic status moderates age-related differences in the brain's functional network organization and anatomy across the adult lifespan. *Proc Natl Acad Sci U S A*. 2018;115(22):E5144–E5153.
32. Arneemann KL, Chen AJ, Novakovic-Agopian T, Gratton C, Nomura EM, D'Esposito M. Functional brain network modularity predicts response to cognitive training after brain injury. *Neurology*. 2015;84(15):1568–1574.
33. Moulder KL, Snider BJ, Mills SL, et al. Dominantly inherited Alzheimer network: Facilitating research and clinical trials. *Alzheimers Res Ther*. 2013;5(5):48.
34. Bateman RJ, Xiong C, Benzinger TL, et al.; Dominantly Inherited Alzheimer Network. Clinical and biomarker changes in

- dominantly inherited Alzheimer's disease. *N Engl J Med.* 2012; 367(9):795–804.
35. Suarez-Calvet M, Araque Caballero MA, Kleinberger G, et al.; Dominantly Inherited Alzheimer Network. Early changes in CSF sTREM2 in dominantly inherited Alzheimer's disease occur after amyloid deposition and neuronal injury. *Sci Transl Med.* 2016;8(369):369ra178.
  36. Landau SM, Mintun MA, Joshi AD, et al.; Alzheimer's Disease Neuroimaging Initiative. Amyloid deposition, hypometabolism, and longitudinal cognitive decline. *Ann Neurol.* 2012;72(4): 578–586.
  37. Petersen RC, Aisen PS, Beckett LA, et al. Alzheimer's disease neuroimaging initiative (ADNI): Clinical characterization. Comparative Study, Multicenter Study, Research Support, N.I.H., Extramural. *Neurology.* 2010;74(3):201–209.
  38. Scholl M, Lockhart SN, Schonhaut DR, et al. PET imaging of tau deposition in the aging human brain. *Neuron.* 2016;89(5): 971–982.
  39. Ikonovic MD, Abrahamson EE, Price JC, Mathis CA, Klunk WE. [F-18]AV-1451 positron emission tomography retention in choroid plexus: More than “off-target” binding. *Ann Neurol.* 2016;80(2):307–308.
  40. Bateman RJ, Benzinger TL, Berry S, et al.; DIAN-TU Pharma Consortium for the Dominantly Inherited Alzheimer Network. The DIAN-TU next generation Alzheimer's prevention trial: Adaptive design and disease progression model. *Alzheimers Dement.* 2017;13(1):8–19.
  41. Storandt M, Balota DA, Aschenbrenner AJ, Morris JC. Clinical and psychological characteristics of the initial cohort of the Dominantly Inherited Alzheimer Network (DIAN). *Neuropsychol.* 2014;28(1):19–29.
  42. Crane PK, Carle A, Gibbons LE, et al.; Alzheimer's Disease Neuroimaging Initiative. Development and assessment of a composite score for memory in the Alzheimer's Disease Neuroimaging Initiative (ADNI). *Brain Imaging Behav.* 2012;6(4): 502–516.
  43. Weiner MW, Veitch DP, Aisen PS, et al.; Alzheimer's Disease Neuroimaging Initiative. Recent publications from the Alzheimer's Disease Neuroimaging Initiative: Reviewing progress toward improved AD clinical trials. *Alzheimers Dement.* 2017;13(4):e1–e85.
  44. Schaefer A, Kong R, Gordon EM, et al. Local-global parcellation of the human cerebral cortex from intrinsic functional connectivity MRI. *Cereb Cortex.* 2017;28(9):3095–3020.
  45. Yeo BT, Krienen FM, Sepulcre J, et al. The organization of the human cerebral cortex estimated by intrinsic functional connectivity. *J Neurophysiol.* 2011;106(3):1125–1165.
  46. Newman ME. Analysis of weighted networks. *Phys Rev E Stat Nonlin Soft Matter Phys.* 2004;70(5 Pt 2):056131.
  47. La Joie R, Visani AV, Baker SL, et al. Prospective longitudinal atrophy in Alzheimer's disease correlates with the intensity and topography of baseline tau-PET. *Sci Transl Med.* 2020;12(524):eaau5732.
  48. Brier MR, Gordon B, Friedrichsen K, et al. Tau and Abeta imaging, CSF measures, and cognition in Alzheimer's disease. *Sci Transl Med.* 2016;8(338):338ra66.
  49. Bateman RJ, Aisen PS, De Strooper B, et al. Autosomal-dominant Alzheimer's disease: A review and proposal for the prevention of Alzheimer's disease. *Alzheimers Res Ther.* 2011;3(1):1.
  50. Gordon BA, Blazey TM, Su Y, et al. Spatial patterns of neuroimaging biomarker change in individuals from families with autosomal dominant Alzheimer's disease: A longitudinal study. *Lancet Neurol.* 2018;17(3):241–250.
  51. Day GS, Musiek ES, Roe CM, et al. Phenotypic similarities between late-onset autosomal dominant and sporadic Alzheimer disease: A single-family case-control study. *JAMA Neurol.* 2016; 73(9):1125–1132.
  52. Brier MR, Thomas JB, Fagan AM, et al. Functional connectivity and graph theory in preclinical Alzheimer's disease. *Neurobiol Aging.* 2014;35(4):757–768.
  53. Bertolero MA, Yeo BTT, Bassett DS, D'Esposito M. A mechanistic model of connector hubs, modularity and cognition. *Nat Hum Behav.* 2018;2(10):765–777.
  54. Ito T, Kulkarni KR, Schultz DH, et al. Cognitive task information is transferred between brain regions via resting-state network topology. *Nat Commun.* 2017;8(1):1027.
  55. Franzmeier N, Hartmann J, Taylor ANW, et al. The left frontal cortex supports reserve in aging by enhancing functional network efficiency. *Alzheimers Res Ther.* 2018;10(1):28.
  56. Franzmeier N, Hartmann JC, Taylor ANW, et al. Left frontal hub connectivity during memory performance supports reserve in aging and mild cognitive impairment. *J Alzheimers Dis.* 2017; 59(4):1381–1392.
  57. Hilger K, Ekman M, Fiebach CJ, Basten U. Intelligence is associated with the modular structure of intrinsic brain networks. *Sci Rep.* 2017;7(1):16088.
  58. Tang W, Jabadi S, Zhu Z, et al. A connectional hub in the rostral anterior cingulate cortex links areas of emotion and cognitive control. *Elife.* 2019;8:e43761.
  59. Arenaza-Urquijo EM, Landeau B, La Joie R, et al. Relationships between years of education and gray matter volume, metabolism and functional connectivity in healthy elders. *Neuroimage.* 2013;83:450–457.
  60. Cole MW, Ito T, Bassett DS, Schultz DH. Activity flow over resting-state networks shapes cognitive task activations. *Nat Neurosci.* 2016;19(12):1718–1726.
  61. Cole MW, Reynolds JR, Power JD, Repovs G, Anticevic A, Braver TS. Multi-task connectivity reveals flexible hubs for adaptive task control. *Nat Neurosci.* 2013;16(9):1348–1355.
  62. Finc K, Bonna K, He X, et al. Dynamic reconfiguration of functional brain networks during working memory training. *Nat Commun.* 2020;11(1):2435.
  63. Dumitrescu L, Mahoney ER, Mukherjee S, et al.; The Alzheimer's Disease Neuroimaging Initiative (ADNI). Genetic variants and functional pathways associated with resilience to Alzheimer's disease. *Brain.* 2020;143(8):2561–2575.
  64. Livingston G, Huntley J, Sommerlad A, et al. Dementia prevention, intervention, and care: 2020 report of the Lancet Commission. *Lancet.* 2020;396(10248):413–446.
  65. Newman ME. Modularity and community structure in networks. *Proc Natl Acad Sci U S A.* 2006;103(23):8577–8582.
  66. Brandes U, Delling D, Gaertler M, et al. On modularity clustering. *IEEE Trans Knowl Data Eng.* 2008;20(2):172–188.
  67. Betzel RF, Bassett DS. Multi-scale brain networks. *Neuroimage.* 2017;160:73–83.
  68. Power JD, Mitra A, Laumann TO, Snyder AZ, Schlaggar BL, Petersen SE. Methods to detect, characterize, and remove motion artifact in resting state fMRI. *Neuroimage.* 2014;84:320–341.
  69. Geerligs L, Tsvetanov KA, Cam C, Henson RN. Challenges in measuring individual differences in functional connectivity using fMRI: The case of healthy aging. *Hum Brain Mapp.* 2017;38(8):4125–4156.
  70. Caballero-Gaudes C, Reynolds RC. Methods for cleaning the BOLD fMRI signal. *Neuroimage.* 2017;154:128–149.
  71. Braun U, Plichta MM, Esslinger C, et al. Test-retest reliability of resting-state connectivity network characteristics using fMRI and graph theoretical measures. *Neuroimage.* 2012;59(2):1404–1412.
  72. Stevens AA, Tappon SC, Garg A, Fair DA. Functional brain network modularity captures inter- and intra-individual variation in working memory capacity. *PLoS One.* 2012;7(1):e30468.